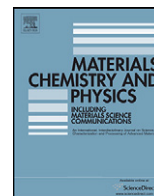




Contents lists available at ScienceDirect

Materials Chemistry and Physics

journal homepage: www.elsevier.com/locate/matchemphys



Stable structure of platinum carbides: A first principles investigation on the structure, elastic, electronic and phonon properties

Venu Mankad^a, Nikita Rathod^{a,b}, Sanjay D. Gupta^a, Sanjeev K. Gupta^a, Prafulla K. Jha^{a,*}

^a Department of Physics, Bhavnagar University, Bhavnagar 364022, India

^b Department of Physics, Vadodra Institute of Engineering, Vadodra 391510, India

ARTICLE INFO

Article history:

Received 25 November 2010

Received in revised form 29 March 2011

Accepted 9 May 2011

Keywords:

First principles

Structure

Elastic

Electronic structure

Phonons

Density of states

ABSTRACT

A comprehensive first principles study of structural, elastic, electronic, phonon and thermodynamical properties of novel metal carbide, platinum carbide (PtC) is reported within the density functional theory scheme. The ground state properties such as lattice constant, elastic constants, bulk modulus, shear modulus and finally the enthalpy of PtC in zinc blende (ZB) and rock-salt (RS) structures are determined. The energy band structure and electron density of states for the two phases of PtC are also presented. Of these phases zinc blende phase of PtC is found stable and phase transition from ZB to RS structure occurs at the pressure of about 37.58 GPa. The phonon dispersion curves and phonon DOS are also presented. All positive phonon modes in phonon dispersion curves of ZB–PtC phase indicate a stable phase for this structure. Within the GGA and harmonic approximation, thermodynamical properties are also investigated. All results reveal that the synthesized PtC would favor ZB phase. The compound is stiffer and ductile in nature.

© 2011 Elsevier B.V. All rights reserved.

1. Introduction

There is currently a growing interest in platinum carbide (PtC) due to the potential of transition metal carbides for basic research and technological applications [1–3]. Platinum carbide belongs to the group known as refractory compounds and it possess promising characteristics such as high stiffness, high hardness, high thermal conductivity and high melting temperature. Most of the earlier experimental and theoretical works focused on groups IV and V transition metal carbides (TMCs) [4–8] due to difficulties in synthesizing the noble metal carbides [8,9]. Recently, Ono et al. [10] have synthesized the PtC at high temperature and high pressure and found that the compound crystallizes in rock-salt (RS or B1) phase with high bulk modulus of 339 GPa. But its structure has been always an issue, particularly in the light of another recently synthesized transition metal compound namely the platinum nitride (PtN) [11]. While, the X-ray diffraction suggests the cubic symmetry with rock-salt type structure for PtN, the zinc blende (ZB) structure is concluded from the Raman spectroscopy for PtN as the first order Raman spectra is forbidden in the case of cubic rock-salt structure. The Raman spectra or phonon spectrum is an important criterion to confirm the structure, particularly for the compounds of large mass difference between anion (Pt) and cation (C or N) as it is difficult to

distinguish between the zinc blende and rock-salt structures solely from the X-ray diffraction intensities [12,13].

The structural stabilities, ground states and electronic properties of PtC compound have been studied recently using theoretical methods [14–17] but the contradiction on its structure is still to be resolved. Li et al. [14] using plane wave pseudo potential based on first principles calculation found zinc blende structure to be mechanically (satisfying the condition for elastic stability) more stable, while Fan et al. [15,16] suggested rock-salt phase of PtC to be more mechanically stable. They found a reasonably good agreement on the compressibility behavior of rock-salt PtC (Rs–PtC) with the experiment. They also suggested that a metastable RS structure may transfer to the more stable ZB structure under certain conditions based on the enthalpy and partial electronic density of states (DOS) [16]. The phase transition pressure from ZB to RS structure using *ab-initio* plane wave pseudopotential density functional theory is reported separately as 52 GPa and 51.7 GPa by Li et al. [14] and Peng et al. [17] respectively. Deligoz et al. [18] found that the ZB phase of PtC transforms to the RS phase at about 42 GPa. Rabah et al. [19] have performed full-potential linearized muffin-tin orbital calculation for different phases of platinum carbide and showed that the PtC is stable in zinc blende phase at zero pressure.

A considerable number of studies have been carried out on the structural and electronic properties of the PtC, but its lattice dynamical properties are still missing despite its importance to confirm the structure. The full phonon properties not only play a significant role in the studies of a wide variety of physical

* Corresponding author. Tel.: +91 2782422650; fax: +91 2782426706.
E-mail addresses: prafullaj@yahoo.com, pkj@bhavuni.edu (P.K. Jha).

properties of solids, such as phase transition, thermal properties, electron–phonon interaction and lattice thermal conduction, but also in the stability of lattice, which is still an important issue to be settled for PtC. Furthermore, the study of the thermodynamical properties of any compound is important to extend our knowledge on their specific behavior when undergoing severe constraints of high pressure and high temperature [20]. This paper focuses on the structural, electronic, elastic, lattice dynamical and thermodynamical properties of rock-salt and zinc blende structures of PtC. To the best of our knowledge, no calculation has been reported to date on the phonon properties of PtC. Further, the present results on the structural, electronic and elastic properties for PtC in RS and ZB phases will provide additional information to the existing data. The phonon properties are obtained using plane wave pseudopotential approach within the framework of density functional perturbation theory (DFPT) [21,22]. The thermodynamical properties including the phonon contribution to the internal energy (ΔE), Gibbs's free energy (ΔF), entropy (S), and the constant-volume specific heat, (C_V) are calculated within the harmonic approximation for ZB-PtC and RS-PtC. The paper is organized as follows: the method of calculation is presented in Section 2 followed by results in Section 3. The conclusion is presented in Section 4.

2. Method of calculation and structure optimization

All calculations in the present study are based on the implementation of plane wave density functional theory (DFT) in the Kohn–Sham framework using ABINIT simulation package [23,24]. The wave functions describe only the valence and the conduction electrons, while the core electrons are taken into account for pseudo-potentials. For the exchange–correlation functional, we have employed the generalized-gradient approximation (GGA) functional developed by Perdew, Burke and Ernzerhof (PBE) [25] since, it is known that GGA gives better results than the simpler local density approximation (LDA) when describing the structural properties of transition metal compounds [26]. The electron–ion interactions are described through the use of Troullier and Martins type pseudo-potentials [27]. A set of convergence tests have been performed in order to choose correctly the mesh of k-points and the cut-off kinetic energy plane waves to start the ground state and linear response calculations. The kinetic energy cut-off for the plane wave basis is set to 30 Ha for both ZB- and RS structures. The Brillouin zone is sampled by $8 \times 8 \times 8$ and $6 \times 6 \times 6$ Monkhorst–Pack mesh of k-points for ZB and RS PtC respectively [21]. Convergence tests prove that the Brillouin zone (BZ) sampling and the kinetic energy cutoff are sufficient to guarantee an excellent convergence. The convergence of the total energy of around 0.0001 Ha, the phonon frequencies by 4 cm^{-1} and the transition pressure by about 1 GPa is ensured. Phonon frequencies are subsequently obtained using the linear response approach [28,29] based on the density functional perturbation theory (DFPT). The expression is obtained from the second derivatives of the total energy with respect to the phonon displacement of atoms or an external electric field.

3. Results and discussion

3.1. Structural properties

At the first stage, the structural optimization of both phases of platinum carbide has been performed under the minimum condition of the total energy and the forces acting on atoms. As a result, we obtained the equilibrium values of the lattice constants and cell volume. The bulk modulus has been computed by minimizing the crystal total energy for different values of the lattice constant by

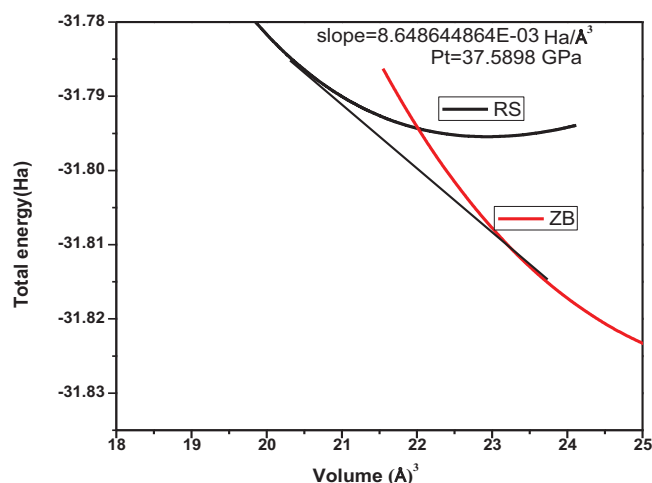


Fig. 1. Total energy per atom (in eV) vs. volume per atom (in \AA^3) for PtC in the rock salt and zinc blende structures and the tangent line whose slope is 23 GPa.

means of Murnaghan equation of state. The calculated total energies of ZB-PtC and RS-PtC as a function of volume together with the experimental data are plotted in Fig. 1. Fig. 1 depicts that the zinc blende phase of PtC has lower energy minimum which occurs at larger lattice constant than the rock salt phase. This suggests that the zinc blende phase is the ground state phase of PtC at zero pressure and it may transform to the rock-salt phase under pressure. The calculated equilibrium lattice constant both places along with the experimental and other theoretical data for PtC is listed in Table 1. The lattice constant obtained in the case of ZB phase agrees better with experiment than the previously reported values. The closure value of lattice constant in ZB phase with experiment further supports that the zinc blende phase is an equilibrium phase at zero pressure. The lattice constant in ZB phase is about 1.5% higher than the RS phase. The calculated phase transition pressure from the slope of the common tangent of energy–volume curves of ZB-PtC and RS-PtC comes out to be 37.58 GPa. In the common tangent technique method, we plot the total energy curves for two phases, the negative of the slope of the common tangent line is taken as the transition pressure. Further, the structural phase transition occurs at a pressure where the difference in enthalpies (ΔH ; $H = E + PV$) of two phases is zero. The state with the lower enthalpy at a given temperature T and pressure P represents the stable phase. Therefore, the crossing point of two curves representing the different structures denotes a first order phase transition with coexisting temperature T_c and pressure P_c . The term due to phonon modes in the free energy has a considerable influence on the location of the phase transition point. Fig. 2 shows the enthalpy as a function of the pressure for PtC. It reveals that the transition pressure from ZB to RS structure takes place at about 37.58 GPa, which is in good agreement with the common tangent calculation presented in Fig. 1. However, the present calculated value on phase transition pressure from both methods is bit low in comparison to the earlier reported values of about 52 GPa [14–17] and almost same as (42 GPa) in Ref. [18]. Obviously, the discrepancy between our data and the previous results is not a serious drawback in the absence of any experimental data, so all data including the present are predictive. Further, it is important to notice that the phase transition pressure 52 GPa reported in Refs. [14,17] reports the lattice constant value quite lower than the present one (4.760 Å) which is off course more close to the experiment (4.814 Å) than all earlier studies. However an analysis that follows from elastic constants and phonon dispersion curves does not suggest for higher phase transi-

Table 1

The elastic constants (in GPa), equilibrium lattice constants a_0 (Å), bulk modulus (B) together with other theoretical and experimental data for PtC in ZB and RS structures.

Material	References	C_{11} (GPa)	C_{12} (GPa)	C_{44} (GPa)	Lattice constant, a_0 (Å)	Bulk modulus, B (GPa)
PtC (ZB)	Present (GGA)	236.668	194.298	88.340	4.760	208.421
	Theory ^a (LDA)	290.2	245.8	42.6	4.678	260.6 ^f
	Theory ^a (GGA)	244.2	206.2	32.8	4.764	218.8
	Theory ^b (GGA)	284	199	70	4.73	227.34 ^f
	Theory ^c (GGA)	289.8	244.6	42.1	4.731	234.79, 265.77
	Theory ^d (LDA)	357.4	226.3	35.1	4.687	270
PtC (RS)	Present (GGA)	271.421	225.29	46.29	4.5097	240.672
	Theory ^a (LDA)	373.6	284.0	47.0	4.425	313.9
	Theory ^a (GGA)	277.8	256.4	51.7	4.506	263.5
	Theory ^b (GGA)	252	271	55	4.49	257
	Theory ^c (GGA)	370.3	283.4	50.2	4.49	267.39, 232.35
	Theory ^d (LDA)	430.87	368.91	66.42	4.427	389.5
	Experimental ^e	–	–	–	4.814	339

^a Ref. [15].

^b Ref. [14].

^c Ref. [17].

^d Ref. [18].

^e Ref. [10].

^f Calculated using available data from the corresponding references.

tion pressure and the present predicted phase transition pressure of about 38 GPa seems quite reasonable.

3.2. Elastic properties

The elastic constants of a solid provide link between the mechanical and dynamical behaviors and provide important information concerning the nature of the forces operating in solids, stability and stiffness of materials. The elastic constants are calculated by treating homogeneous strain within the framework of linear response theory [30] and listed in Table 1 along with other theoretical data for both ZB and RS PtC. For the elastic constants, at present there are no experimental data to compare with our results but they seem to be in reasonable order with other available theoretical data obtained using GGA. It is important to note that the elastic constant data listed in table are highly diverse and hence only on the basis of elastic constants data it is difficult to comment on the success of method. However, the good agreement in the case of lattice constant and other properties in what follows give confidence to the present approach. The traditional mechanical stability conditions of the elastic constants are known to be $C_{11} - C_{12} > 0$, $C_{11} > 0$, $C_{44} > 0$, $C_{11} + 2C_{12} > 0$ and $C_{12} < B < C_{11}$. The present results for elastic constants in Table 1 satisfy these stability conditions.

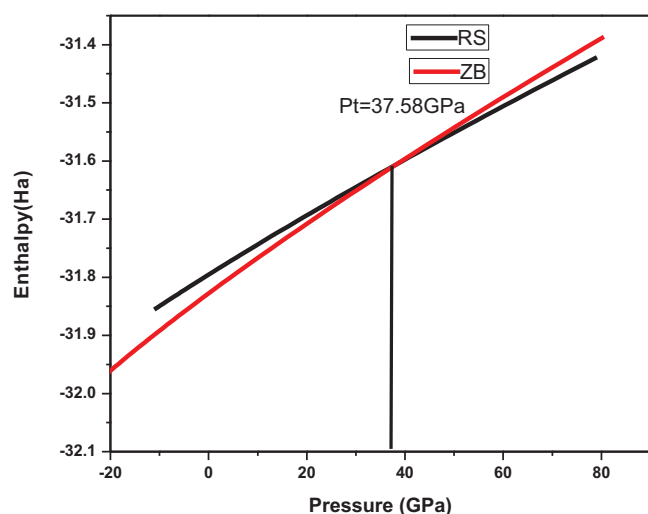


Fig. 2. Estimation of phase transition pressure from ZB to RS structure by enthalpy method.

It is noticed that the C_{12} is closer to C_{11} , i.e. difference between C_{11} and C_{12} is not reasonably high for both phases, however, it is almost 1.5 times higher in the RS-PtC than ZB-PtC, which implies that the ZB-PtC phase may be unstable against a small homogeneous deformations. Further, the velocity of a longitudinal wave in the [1 0 0] direction is much larger than the one of a shear wave as C_{44} is much lower than C_{11} . The low value of $C_{11} - C_{12}$ and large value of $C_{11} - C_{44}$ direct for a phase transition with a small or moderate deformation (pressure) and hence a phase transition pressure of about 37.58 GPa obtained from enthalpy and common tangent method (Figs. 1 and 2) seems to be reasonable.

The Zener anisotropy factor A , Poisson's ratio ν , Young's modulus Y , polycrystalline and tetragonal shear modulus G_v and C' respectively are the most interesting elastic properties for any applications, particularly for their hardness. These quantities are calculated in terms of the computed data using the following relations [30–32].

$$A = \frac{2C_{44}}{C_{11} - C_{12}} \quad (1)$$

$$\nu = \left[\frac{(B - (2/3)G)}{(B + (1/3)G)} \right] \quad (2)$$

$$Y = \frac{9GB}{G + 3B} \quad (3)$$

$$C' = \frac{C_{11} - C_{12}}{2} \quad (4)$$

where $G = (G_v + G_R/2)$ is the isotropic shear modulus. G_v is the Voigt's shear modulus or polycrystalline shear modulus corresponding to the upper bound of G values and G_R the Reuss's shear modulus corresponding to the lower bound of G values and they can be written as $G_v = (C_{11} - C_{12} + 3C_{44})/5$ and $5/G_R = 4/(C_{11} - C_{12}) + 3/C_{44}$ and bulk modulus B is $(C_{11} + 2C_{12})/3$. The calculated bulk modulus for PtC in both phases is presented in Table 1. The lower value in comparison to the experiment is an inherent property of GGA, which is known to underestimate the bulk modulus.

The calculated Zener anisotropy factor, Poisson's ratio, Young's modulus, and both polycrystalline and tetragonal shear modulus in both structures obtained using above expressions, are found to be in order and presented in Table 2. This could not be compared with experimental data as they are not available so. However, these are derived values obtained from the elastic constants data and their accuracy strongly depends on them presented in Table 1.

Table 2
The calculated Zener anisotropy factor (A), Poisson's ratio (ν), Young's modulus (Y), shear modulus (C') and polycrystalline shear modulus (G) together with other theoretical data for PtC in ZB and RS structures.

Material	References	Anisotropy factor (A)	Poisson's ratio (ν)	Young's modulus (Y) GPa	Shear modulus (C') GPa	Polycrystalline shear modulus (G)
PtC (ZB)	Present (GGA)	4.169	0.3646	167.90	21.18	61.47
	Theory ^a (LDA)	1.9189 ^f	0.4578 ^f	93.30	32.40	34.44 ^f
	Theory ^a (GGA)	1.7263 ^f	0.440 ^f	74.80	25.90	27.16 ^f
	Theory ^b (GGA)	0.535	0.420	128.22	50.30	47.28 ^f
	Present (GGA)	2.0073	0.4268	128.22	23.06	37.00
PtC (RS)	Theory ^a (LDA)	1.0491 ^f	0.4299 ^f	131.3	45.9	46.12 ^f
	Theory ^a (GGA)	4.8317	0.4358 ^f	90.0	10.7	31.20
	Theory ^b (LDA)	2.14	0.4358 ^f	140.82	48.7	52.24 ^f
	Theory ^c (LDA)	1.0491	0.430	131.8	44.8	46.1
	Theory ^d (GGA)	5.400	0.440	101.4	10.7	35.3

^a Ref. [15].

^b Ref. [18].

^c Ref. [15].

^f Calculated using available data from the corresponding reference.

Table 2 depicts that the PtC is an elastically highly anisotropic compound as its Zener anisotropy is quite high. This high value of Zener anisotropy factor can be responsible for giving rise the tangential force acting on screw dislocations and resulting into the cross slip pinning process [33–35]. As the PtC is elastically anisotropic we have used the value of polycrystalline shear modulus instead of isotropic shear modulus to calculate Poisson's ratio and Young's modulus. The value of Poisson's ratio closure to 0.36 indicates that the interatomic forces are predominantly central forces in PtC in both structures [34,35]. The high value of Young's modulus, which is a measure of the stiffness, suggests that the PtC is a stiffer compound. Further a very high value of B/G ratio suggests that the PtC behaves in a ductile manner [36,37].

The discrepancy in the case of Young's modulus; Poisson's ratio and anisotropic factor with other reported values can be attributed to the different formula used in the calculation [18]. For example, in the calculation of Young's modulus, we use the polycrystalline shear modulus instead of simple isotropic shear modulus. This is justified as the compound is highly anisotropic.

3.3. Electronic structure

In order to gain insight into the electronic and phase stability of PtC the energy band structure along with electronic density of states (DOS) for ZB and RS-PtC is presented in Figs. 3 and 4 respectively. Both structures show the metallic nature as there is no gap near the Fermi level. Our results for band structures and DOS are similar to other calculations [14,15,18]. In the case of ZB-PtC, Fermi level lies higher than the centre of antibonding zone, in contrast to the carbides of metals of group IV and V where the Fermi level lies between the bonding states zone and antibonding states zone [9,37]. This implies that the antibonding zone is fully occupied in PtC and is responsible for the decrease in the stability of the phase. These figures reveal an interesting and remarkable feature about the position of the Fermi energy; E_F in DOS. The Fermi energy, E_F , falls on a shoulder of a small peak in the DOS curve in the case of RS-PtC and in a gap region in the case of ZB-PtC. A strong correlation between structure stability and position of the Fermi level in the DOS suggests that if E_F falls in pseudo gap that separates bonding states from antibonding states in a particular phase, the phase will become more stable. Thus DOS indicates that the ZB-phase for PtC is stable. It is also known that the topological changes of the Fermi surfaces can lead to anomalies in phonon frequencies and in some cases to phonon softening and structural transitions [38–40]. Therefore a phonon calculation is vital for this compound to find the role of phonons in the stability of PtC.

3.4. Dynamical and thermodynamical properties

In order to get an idea about the behavior of phonons and role played by them in the stability of the structures and phase transformation in PtC, we have calculated the phonon dispersion curves (PDC) and phonon density of states for both zinc blende and rock-salt phases of PtC. The calculated PDC along major symmetry directions of the BZ together with the corresponding phonon density of states are presented in Figs. 5 and 6 for ZB-PtC and RS-PtC

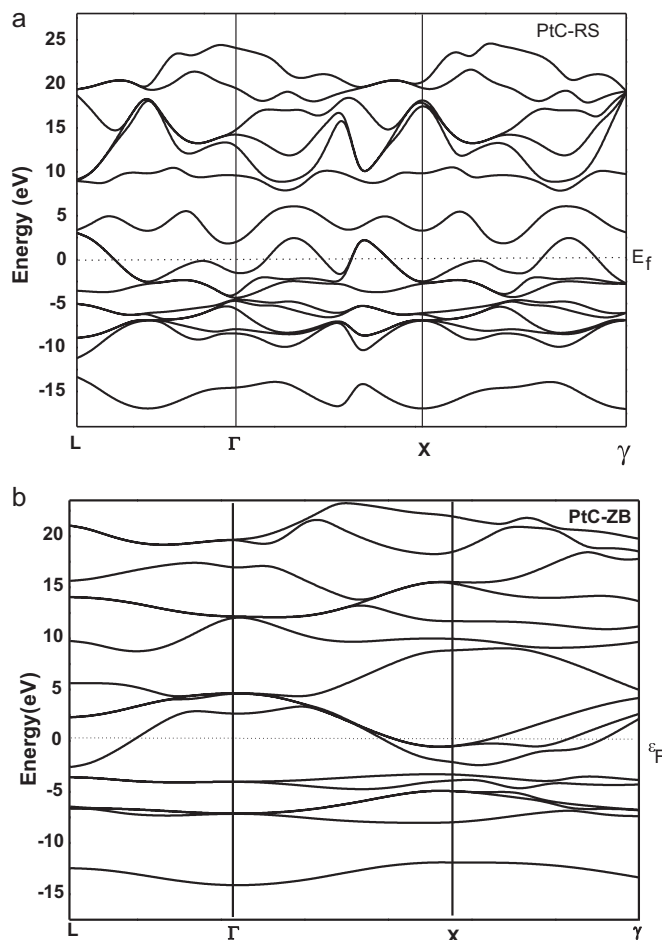


Fig. 3. (a) Energy bands of zinc blende PtC along symmetry direction near the Fermi energy (located at $E=0$). (b) Energy bands of rock-salt PtC along symmetry direction near the Fermi energy (located at $E=0$).

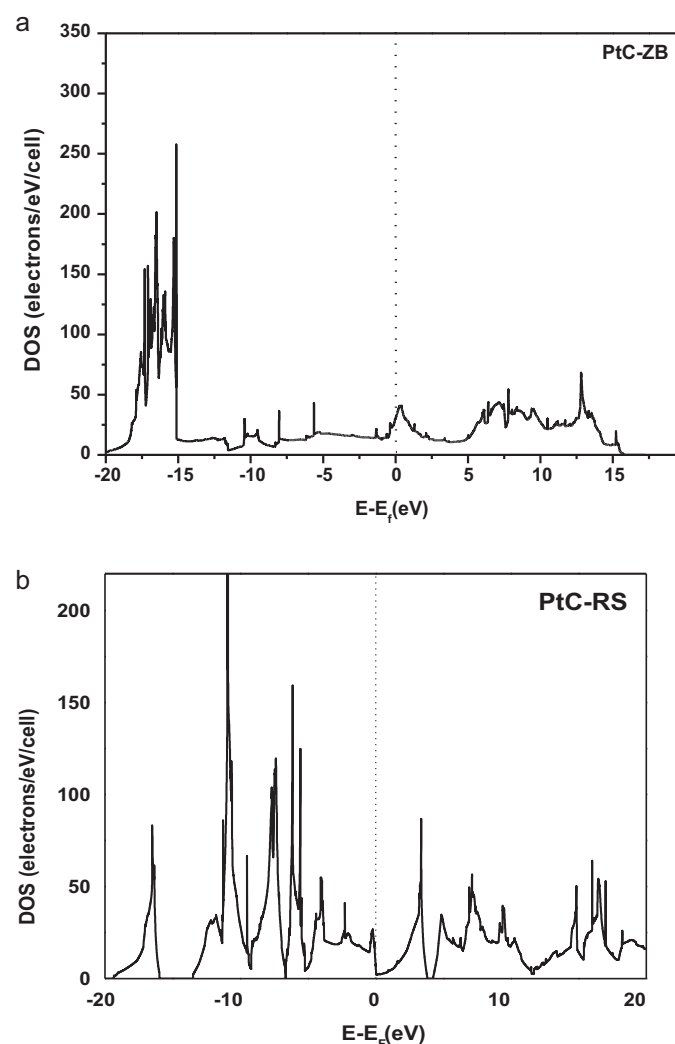


Fig. 4. (a) Electronic density of states and of zinc blende PtC. The Fermi level is set to be 0 eV. (b) Electronic density of states and of rock-salt PtC. The Fermi level is set to be 0 eV.

respectively. As the cubic structure has two atoms in the primitive unit cell there are 6 phonon branches. Figs. 5 and 6 reveal that the all phonon modes are positive in the phonon dispersion curves of ZB-PtC, while the PDC of RS-PtC consists of many negative and unstable phonon modes. This reflects and confirms that the ZB structure of PtC is dynamically stable. As, the ZB-PtC is dynamically

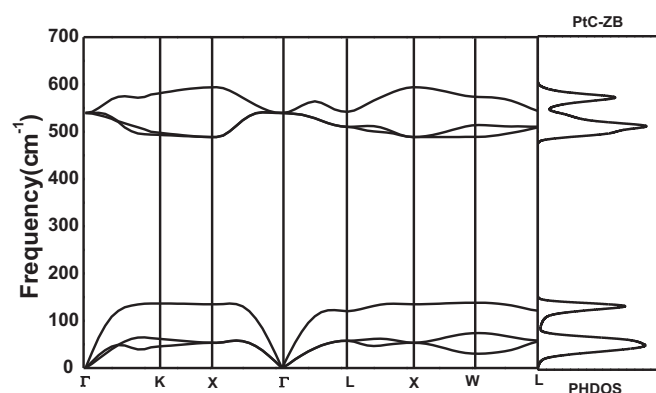


Fig. 5. Phonon dispersion curve for zinc-blende PtC along the main symmetry direction in BZ along with one phonon density of states.

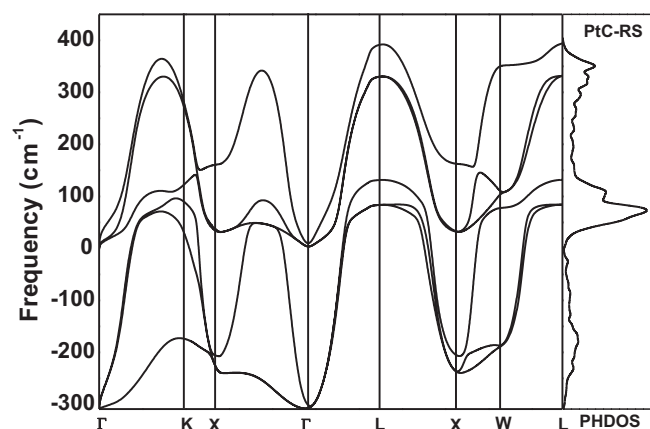


Fig. 6. Phonon dispersion curve for rock-salt PtC structure along the main symmetry direction in BZ along with one phonon density of states.

stable phase, we focus our attention to phonon dispersion curves of ZB-PtC. The presence of imaginary frequencies in the phonon dispersion curves of RS-PtC (Fig. 6) supports the dynamical instability of RS-PtC phase. Similar phonon dispersion curves have been earlier reported for unstable RS-LaN [41]. It is seen from Fig. 5 that the large difference in mass between anions and cations results in large gap and hence the divergence ($\approx 300 \text{ cm}^{-1}$) between the acoustic and optical phonon branches is very clear in stable ZB-PtC which is consistent with the similar compound RhN [35]. The LO/TO splitting is zero and triply degenerates at the symmetry point Γ (zone centre), suggesting metallic nature of PtC. The phonon density of states is an important dynamical property as its computation needs frequencies in the entire Brillouin Zone and can be defined as [20,39,42]

$$g(\omega) = \frac{1}{N} \int_{\text{BZ}} \sum_j \delta[\omega - \omega_j(\vec{q}) d\vec{q}] \quad (5)$$

where N is a normalization constant that $\int g(\omega) d\omega = 1$. $g(\omega) d\omega$ is the ratio of the number of eigen states in the frequency interval (ω , $\omega + d\omega$) to the total number of eigen states. $\omega_j(\vec{q})$ is the phonon modes. The phonon DOS presented in the right panel of Fig. 5 depicts all main features of dispersion. The phonon gap can be easily seen on the phonon DOS plot. The sharp peaks in the phonon DOS correspond to the flat modes of the phonon dispersion curves which belong to both optic and acoustic branches. Similar to the dispersion curves, there is a gap between the optic and acoustic branches. However, contrary to this there is no gap between the optic and acoustic branches in the case of rock salt phase as can be seen from the phonon DOS plot. Once, it is clear from the phonon dispersion curves regarding the stability of the structure, we turn our attention to understand the mechanism of phase transition from phonon dispersion. It is recognized that the softening of transverse acoustic (TA) phonon mode at the zone boundary point X or L in the Brillouin zone drives the structural phase transition [43]. Further, it is known from the theory [44] that the small difference in C_{11} and C_{12} is responsible for the phase transition and should be reflected in PDC in terms of softening or instability of TA phonon mode. In order to shed light on the pressure dependence behavior of PtC and its relations to the phase transition we have also calculated the phonon dispersion curves for the stable ZB-PtC at two pressures below the phase transition pressure of 37.58 GPa. However, we present only the PDC of ZB-PtC (Fig. 7) at 16 GPa which clearly shows the softening/instability of TA phonon mode at zone boundary points. It is thus clear from this fact that the phase transition is driven by TA phonon mode. This reflects that the ZB-PtC which is a stable phase will undergo the phase transition at lower pressure.

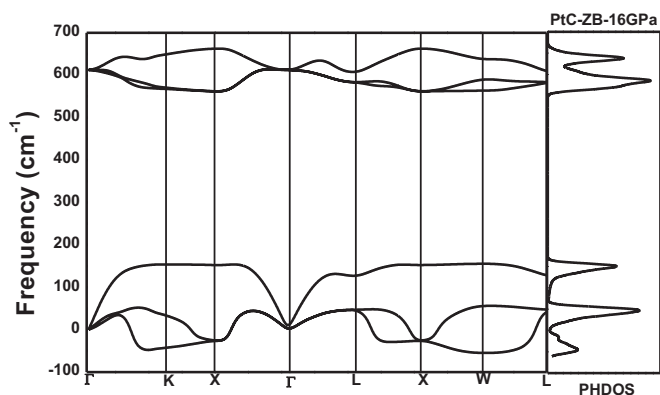


Fig. 7. Phonon dispersion curves along the main symmetry directions and one phonon density of states for zinc blende-PtC at 16 GPa.

Hence, the phase transition pressure of 40 GPa lower than the previously reported values of 42–52 GPa to transform from ZB to RS structure for PtC obtained from the enthalpy in the present study seems quite reasonable and justifiable.

The knowledge of the entire phonon dispersion curves and DOS makes possible the evaluation of several critical thermodynamical quantities and of the relative stability of the system among different crystal structures. The thermodynamic properties such as Gibbs free energy ΔF , internal energy ΔE , entropy S , and constant volume specific heat C_v with temperature for ZB and RS-PtC are calculated

using the expressions within the quasi harmonic approximation [39].

$$\Delta F = 3nNk_B T \int_0^{\omega_L} \ln \left\{ 2 \sinh \frac{\hbar\omega}{2k_B T} \right\} g(\omega) d\omega \quad (6)$$

$$\Delta E = 3nN \frac{\hbar}{2} \int_0^{\omega_L} \omega \coth \left(\frac{\hbar\omega}{2k_B T} \right) g(\omega) d\omega \quad (7)$$

$$S = 3nNk_B \int_0^{\omega_L} \left[\frac{\hbar\omega}{2k_B T} \coth \frac{\hbar\omega}{2k_B T} - \ln \left\{ 2 \sinh \frac{\hbar\omega}{2k_B T} \right\} \right] g(\omega) d\omega \quad (8)$$

$$C_v = 3nNk_B \int_0^{\omega_L} \left(\frac{\hbar\omega}{2k_B T} \right)^2 \coth^2 \left(\frac{\hbar\omega}{2k_B T} \right) g(\omega) d\omega \quad (9)$$

where K_B is the Boltzman constant, n is the number of atoms per unit cell, N is the number of unit cells, ω_{\max} is the highest phonon frequency and ω is the phonon frequency. In Fig. 8(a) we present the variation of free energy with temperature which reveals that the overall profiles for both phases are similar and free energy decreases with increasing temperature. The computed temperature dependent entropy is presented in Fig. 8(b) and similar trend is observed for both phases. However, the difference in entropies increases with the increase in temperature. Fig. 8(c) presents the lattice specific heat at constant volume for PtC in both phases and reveals that the specific heat behavior approaches the Dulong and Petit limit at high temperature. At lower temperatures (<1000 K) the constant volume specific heat, C_v , value for ZB-PtC is lower than RS-PtC. The figure clearly shows that the C_v does not follow the Debye's specific heat formula at low temperature in the case of RS-

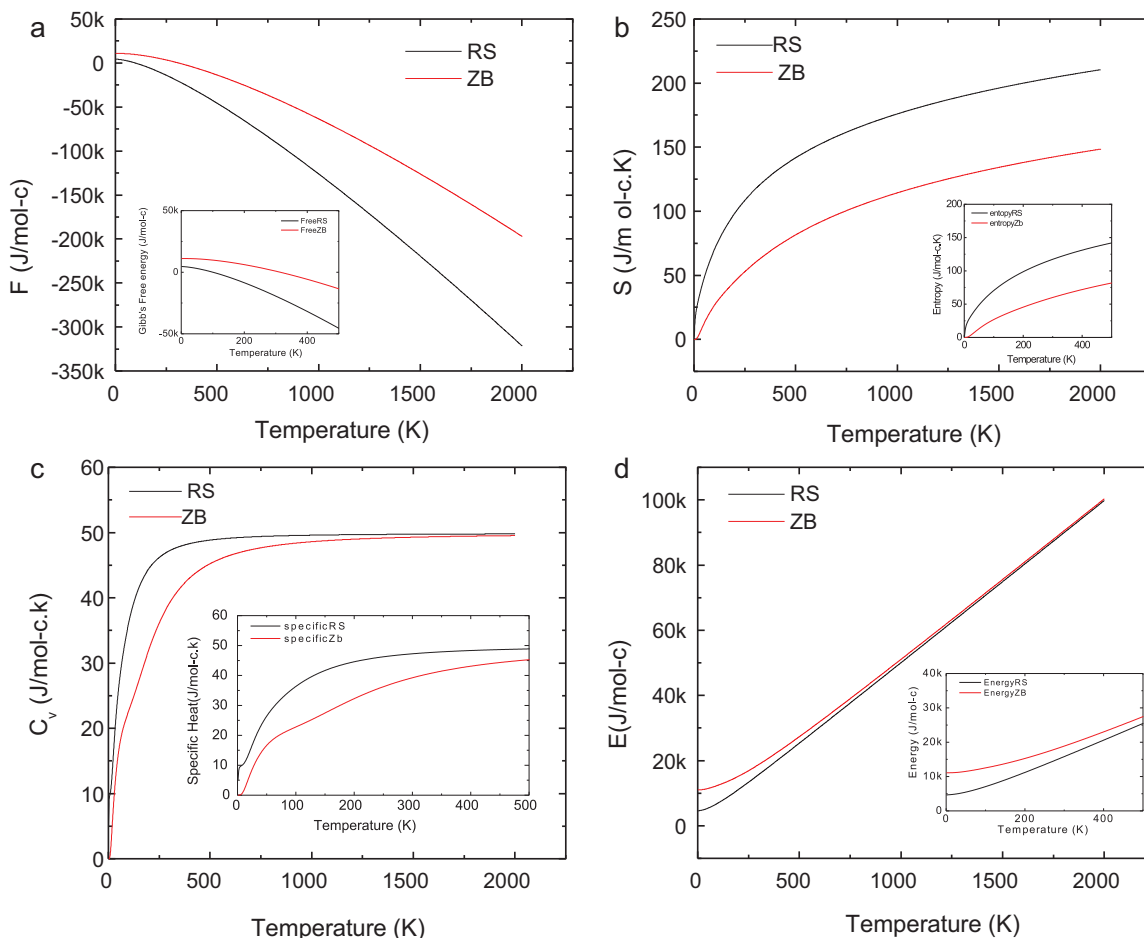


Fig. 8. Calculated Gibbs free energy, enthalpy, constant volume specific heat and internal energy.

PtC, which is quite obvious due to unstable acoustic phonon modes. Fig. 8(d) shows the gradual increase of internal energy ΔE , and it approaches to the same value at high temperature for both structures and increases almost linearly. The zero temperature values of internal and free energies do not vanish due to zero point motion [42].

4. Conclusions

In summary, we have investigated the structural, elastic, electronic and dynamical properties of platinum carbide using *ab-initio* plane wave pseudopotentials density functional theory for zinc blende and rock salt phases of PtC. On the basis of usual condition of equal enthalpy and common tangent methods, we found that the phase transition from zinc blende to rock salt structure occurs at about 37.58 GPa. Our phonon calculation based on density perturbation theory using linear response theory suggests that the ZB-PtC is a stable phase as all the phonon modes in the phonon dispersion curves are positive in contrast to the RS-PtC for which many phonon modes are negative, a sign of unstable structure. Even a pressure of about 16 GPa leads to the unstable modes and hence the lower value of phase transition pressure, 37.58 GPa in comparison to the earlier reported higher transition pressure seems reasonable and justified. Within the harmonic approximation phonon properties are used to determine the thermodynamic properties such as Gibbs free energy, internal energy, entropy and constant-volume specific heat for PtC in both considered phases. The zero pressure elastic constants and their related quantities such as bulk modulus, shear modulus, Young's modulus, anisotropy factor have been also calculated. The compound is highly anisotropic, stiffer and ductile in nature. The results could not be compared with the experiments. The main aim of the present work was to remove an existing ambiguity with respect to the stability of the phases and we have been able to bring out that the zinc blende phase is the stable phase for PtC at zero pressure. The NaCl-like rocksalt structure may be stable only at high pressure. We hope that the results will be tested in future, experimentally in order to confirm their reliability and the knowledge of the present parameters is especially important for the future use of this material for fundamental as well as application.

Acknowledgements

This work is supported by the University Grants Commission (UGC) and Department of Science and Technology (DST), Govt. of India. The computations are performed using PAWAN at the Department of Physics, Bhavnagar University, Bhavnagar under project grant of DST, Govt. of India.

References

- [1] E.K. Storms, The Refractory Carbides, Academic, New York, 1967.
- [2] L.E. Toth, Transition Metal Carbides and Nitrides, Academic, New York, 1971.
- [3] A.L. Ivanovskii, Russ. Chem. Rev. 78 (2009) 303.
- [4] P. Blaha, K. Schwarz, Int. J. Quant. Chem. XXIII (1983) 1535.
- [5] K. Schwarz, Solid State Mater. Sci. 13 (1987) 211.
- [6] S.H. Jhi, J. Ihm, S.G. Louie, M.L. Cohen, Nature (Lond.) 399 (1999) 132.
- [7] M. Sahnoun, C. Daul, M. Driz, J.C. Parlebas, C. Demangeat, Comput. Mater. Sci. 33 (2005) 175.
- [8] X.J. Chen, V.V. Struzhkin, Z.G. Wu, M. Somayazulu, J. Qian, S. Kung, A.N. Christensen, Y.S. Zhao, R.E. Cohen, H.K. Mao, R.J. Hemley, Proc. Natl. Acad. Sci. U.S.A. 102 (2005) 3198.
- [9] J.C. Grossman, A. Mizel, M. Cote, M.L. Cohen, S.G. Louie, Phys. Rev. B 60 (1999) 6343.
- [10] S. Ono, T. Kikegawa, Y. Ohishi, Solid State Commun. 133 (2005) 55.
- [11] E. Gregoryanz, C. Sanloup, M. Somayazulu, J. Badro, G. Flquet, H.K. Mao, R.J. Hemley, Nat. Mater. 5 (2004) 294.
- [12] M.B. Kanoun, S. Goumri-Said, Phys. Rev. B 72 (2005) 113103.
- [13] B.R. Sahu, L. Kleinman, Phys. Rev. B 71 (2005) 041101(R).
- [14] L. Li, W. Yu, C. Jin, J. Phys. Condens. Matter 17 (2005) 5965.
- [15] C.Z. Fan, L.L. Sun, Y.X. Wang, R.P. Liu, S.Y. Zeng, W.K. Wang, Physica B 381 (2006) 174.
- [16] C.Z. Fan, S.Y. Zeng, Z.J. Zhan, R.P. Liu, W.K. Wang, P. Zhang, Y.G. Yao, Appl. Phys. Lett. 89 (2006) 071913.
- [17] F. Peng, H.Z. Fu, X.D. Yang, Solid State Commun. 145 (2008) 91.
- [18] E. Deligoz, Y.O. Ciftci, P.T. Ochym, K. Gokoglu, Mater. Chem. Phys. 111 (2008) 29.
- [19] M. Rabah, D. Rached, M. Ameri, R. Khenata, A. Zenati, N. Moulay, Phys. Chem. Solids 69 (2008) 2907.
- [20] P.K. Jha, Phys. Rev. B 72 (2005) 214502; P.K. Jha, S.P. Sanyal, Physica C 261 (1996) 259; P.K. Jha, S.P. Sanyal, Physica C 271 (1996) 6.
- [21] H.J. Monhorst, J.D. Pack, Phys. Rev. B 13 (1976) 5188.
- [22] P. Giannozzi, S. de Gironcoli, P. Pavone, S. Baroni, Phys. Rev. B 43 (1991) 7231; S. Baroni, P. Giannozzi, A. Testa, Phys. Rev. Lett. 58 (1987) 1861.
- [23] X. Gonze, J.M. Beuken, R. Caracas, F. Detraux, M. Fuchs, G.-M. Rignanese, L. Sindic, M. Verstraete, G. Zerah, F. Jollet, M. Torrent, A. Roy, M. Mikami, Ph. Ghosez, J.Y. Raty, D.C. Allan, Comput. Mater. Sci. 25 (2002) 478.
- [24] The Abinit Code is a common project of the University Catholique de Louvain, Corning Incorporated, and other contributions <http://www.abinit.org>.
- [25] J.P. Perdew, K. Burke, M. Ernzerhof, Phys. Rev. Lett. 77 (1996) 3865.
- [26] P. Raybaud, G. Kresse, J. Hafner, H. Toulhoat, J. Phys. Condens. Matter 9 (1997) 11085.
- [27] N. Troullier, J.L. Martin, Phys. Rev. B 13 (1976) 5188.
- [28] X. Gonze, C. Lee, Phys. Rev. B 55 (1997) 10355.
- [29] H. Shimizu, M. Shirai, Suzuki, J. Phys. Soc. 66 (1997) 3147.
- [30] D.R. Hamann, X. Wu, K.M. Rabe, D. Vanderbilt, Phys. Rev. B 71 (2005) 035117.
- [31] I. Johnston, G. Keller, R. Rollins, S. Spickelmire, Solid State Physics Simulations, The Constortium for Upper-Level Physics Software, John Wiley, New York, 1996.
- [32] B. Mayer, H. Anton, E. Bott, M. Methfessel, J. Sticht, J. Harris, P.C. Schmidt, Intermetallics 11 (2003) 23.
- [33] H. Fu, D. Li, F. Peng, T. Gao, X. Cheng, Comput. Mater. Sci. 44 (2008) 774.
- [34] M.H. Yoo, Scr. Metall. 20 (1986) 915.
- [35] E. Deligoz, K. Colakoglu, Y.O. Ciftci, J. Mater. Sci. 45 (2010) 3729.
- [36] I.R. Shein, A.L. Ivanovskii, J. Phys. Condens. Matter 20 (2008) 415218.
- [37] F. Lay, P. Henes, P.E. Schmid, R. Sanjines, M. Diserens, C. Wiemer, Surf. Coat. Technol. 284 (1999) 120.
- [38] W.A. Groshans, Y.K. Vohra, W.B. Holzapfel, Phys. Rev. Lett. 49 (1982) 1572.
- [39] L. Dangens, J. Phys. F 8 (1978) 2093.
- [40] J.E. Schirber, in: K.D. Timmerhans, M.S. Barber (Eds.), High pressure Science and Technology, vol. 1, Plenum, New York, 1979, p. 130.
- [41] G. Gokoglu, A. Erkisi, Solid State Commun. 147 (2008) 221.
- [42] C. Lee, X. Gonze, Phys. Rev. B 51 (1995) 8610.
- [43] N. Hamaya, Y. Sakamoto, H. Fujihisa, Y. Fujii, K. Takemura, T. Kikegawa, O. Shimomura, J. Phys. Condens. Matter 5 (1993) L369.
- [44] P. Soderlind, O. Erikson, J.M. Wills, A.M. Boring, Phys. Rev. B 48 (1993) 9306.